# Annealing effects and Te mixing in CdTe/CdS heterojunctions

Y. L. Soo, S. Huang, and Y. H. Kao[a)]
*Department of Physics, State University of New York at Buffalo, Amherst, New York 14260*

A. D. Compaan
*Department of Physics and Astronomy, The University of Toledo, Toledo, Ohio 43606*

(Received 6 July 1998; accepted for publication 12 November 1998)

Angular dependence of x-ray fluorescence techniques have been employed to investigate the effects of thermal annealing at various temperatures ranging from 340 to 387 °C on a series of CdTe/CdS heterojunctions. Changes in depth profiles of Te and Cd atoms in the CdS layer as a result of heat treatment has been observed. A simple model is proposed for comparison of the ratio of Te $K\alpha$ to Cd $K\alpha$ fluorescence yield at different annealing temperatures. Our results suggest that the concentration of migrated Te atoms in the CdS layer increases with the annealing temperature, and the Te/Cd ratio in the CdS layer could even become greater than that in CdTe with annealing temperatures higher than 370 °C. © *1999 American Institute of Physics.* [S0003-6951(99)04202-3]

Heterojunctions of the *p*-type direct-gap semiconductor CdTe and its *n*-type CdS window partner have shown a promisingly high light-conversion efficiency of 15.8% as well as enhanced short-wavelength response, low series resistance, stability, and high radiation tolerance.[1,2] In view of these outstanding properties, this material is widely considered to be very useful for the next-generation photovoltaic (PV) technologies. For further improvement of the quality of this PV material, it is desirable to control factors which may adversely affect cell performance such as interface morphology. Although some interdiffusion and blurring of the interface may be advantageous and help to relieve the large (about 10%) lattice mismatch between CdS and CdTe, microstructural defects will likely cause local traps and undesirable recombination or scattering of charge carriers. This is especially critical when it occurs in the photogenerated carrier region near the heterojunction.

An effect of technical as well as fundamental interest is the change of heterojunction quality as a result of thermal treatment. The light-conversion efficiency of CdTe/CdS heterojunction solar cells has been known to vary with thermal annealing.[3] We have found that for rf-sputtered cells, the efficiency rises from less than 1% for as-deposited cells and remains low until annealing at temperatures above 370 °C in the presence of $CdCl_2$. It is conceivable that such an efficiency change could originate from either structural or compositional variations in the annealed heterojunctions, such as due to intermixing of Te or Cd across the junction interface. For this reason, techniques of angular dependence of x-ray fluorescence (ADXRF) have been employed in the present work to investigate the changes in spatial distribution of Te and Cd atoms in a series of CdTe/CdS heterojunctions subjected to different temperatures of thermal annealing.

The intensity of fluorescence yield (FY) of our system can be expressed as[4,5]

$$I_{\mathrm{FY}} \propto \int dz \left( -\frac{dS_z(z)}{dz} \right) \Phi(z), \tag{1}$$

where $S_z$ is the $z$ component (perpendicular to the interfaces) of the Poynting vector, and $\Phi(z)$ is the density profile of the fluorescent atoms in the $z$ direction. Thus, by measuring the FY intensity, it is possible to learn about the depth profile of selected atoms in the compound material.

Samples of the CdTe/CdS heterojunction with CdTe and CdS layer thickness around 200 Å were prepared by rf planar magnetron sputtering of the thin-film materials under the same deposition conditions as those in a previously reported solar cell with an efficiency of 11.6%.[6] The sputter depositions were performed at 280 °C. Subsequent annealing treatments were carried out at temperatures up to 387 °C for 30 min in dry air and equilibrium vapors of $CdCl_2$. The typical CdTe solar cell has a superstate structure with soda-lime-glass/$SnO_2$:F/CdS/CdTe/back contact. The bilayer films studied here were sputtered onto borosilicate glass with either the ''normal'' sequence as above or the ''inverted'' sequence: glass/CdTe/CdS. For the inverted sequence, x-ray fluorescence was measured with incident photons entering the samples through the CdS top layer.

The ADXRF measurements were performed at beamline X3B1 at the National Synchrotron Light Source at Brookhaven National Laboratory, and some experimental details have been reported recently.[7] Incident photon energy of 31.9 keV was selected by using a Si(111) double-crystal monochromator. A two-axis goniometer with angular resolution of 0.001° was used to rotate the sample and thus control the grazing incidence angle $\theta$ between the incident x-ray beam and the film surface. For a precise sample alignment, a selected angle say $\theta = 0.07°$ was first determined accurately from specular reflectivity measurements with an Ar-flowing ionization chamber, and this angle was then used as a reference for defining other incidence angles. The x-ray fluorescence photons from irradiated samples were collected using a solid-state Si(Li) detector calibrated with an energy resolution of 175 eV at the energy of Mn $K\alpha$ emission (5.899 keV). The x-ray fluorescence spectra were obtained by using a multichannel pulse-height analyzer and the intensities of Cd $K\alpha$ at 23.174 keV and Te $K\alpha$ at 27.472 keV were obtained by curve fitting the spectra with Gaussian peaks and a

a)Electronic mail: yhk@acsu.buffalo.edu

 

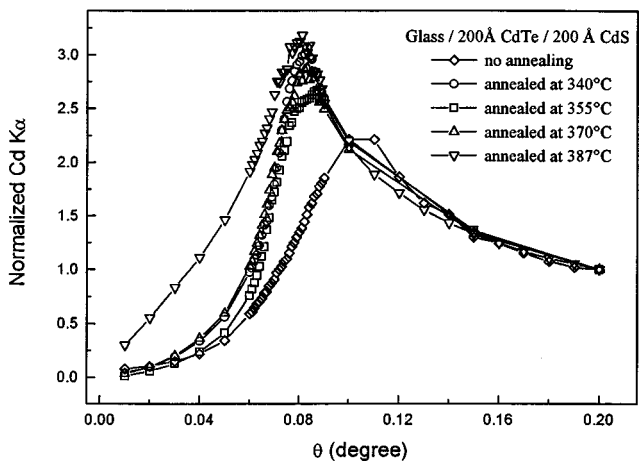


FIG. 1. Angular dependence of Cd $K\alpha$ fluorescence intensity normalized to its value at $\theta = 0.2°$ in each sample for glass/200 Å–CdTe/200 Å–CdS inverted heterojunctions.

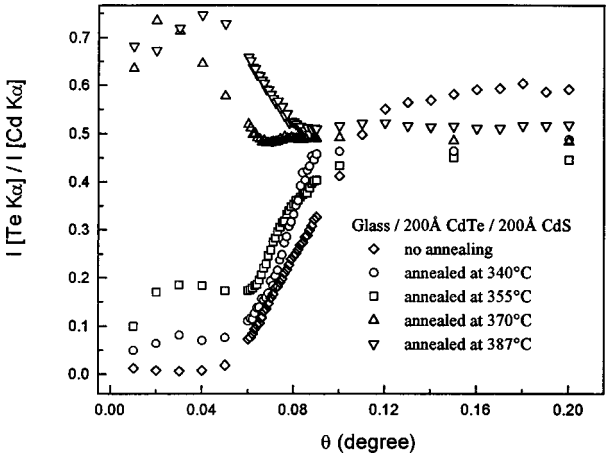


FIG. 3. Angular dependence of Te $K\alpha$/Cd $K\alpha$ FY ratio for glass/200 Å–CdTe/200 Å–CdS inverted heterojunction samples.

constant background. The Cd $K\alpha$ and Te $K\alpha$ fluorescence intensities are all normalized to the Cd $K\alpha$ intensity at $\theta = 0.2°$ for each sample. The ADXRF results are shown in Figs. 1 and 2.

From Fig. 1 it can be seen that at low incidence angles (below 0.07°) the Cd $K\alpha$ FY intensity for the annealed samples increases more rapidly than the unannealed sample. At low angles (below the critical angle) as the incident x-ray penetrates deeper (increasing $z$) into the material with increasing $\theta$, a higher rate of FY intensity increase thus corresponds to a higher concentration of the fluorescent atoms [see Eq. (1)] present near the sample surface. Hence, there are more Cd atoms present near the CdS top surface after heat treatment. It perhaps should be noted that changes in the Cd depth profile are similar for samples annealed between 340 and 370 °C, but a large change was found with a sample annealed at 387 °C. In this analysis, we have taken into account possible changes in the angular dependence of Cd FY due to different thickness values of the CdS and CdTe layers, which were determined accurately from our measurements of grazing incidence x-ray scattering.[8] The large variation between samples annealed at 370 and 387 °C cannot be attributed to the size effect. On the other hand, heat treatment with $CdCl_2$ might leave some residual Cd near the sample surface, and this effect could also be temperature dependent.

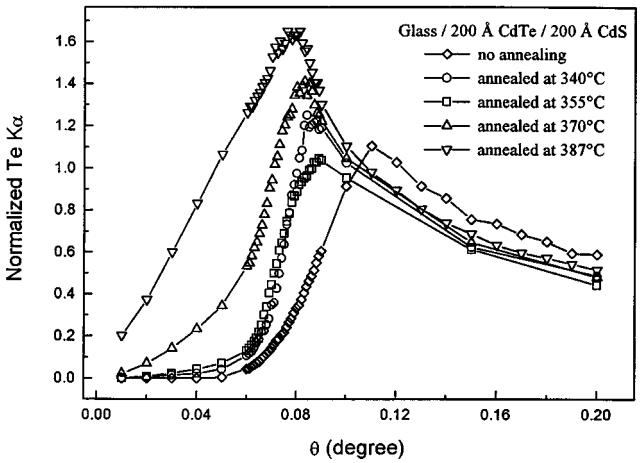


FIG. 2. Angular dependence of Te $K\alpha$ fluorescence intensity normalized to the Cd $K\alpha$ intensity at $\theta = 0.2°$ in each sample for glass/200 Å–CdTe/200 Å–CdS inverted heterojunctions.

The results of Te FY are shown in Fig. 2. In comparison with the increase in Cd FY intensity at low incident angles shown in Fig. 1, the angular dependence of Te FY increases more rapidly with increasing annealing temperature than Cd. This indicates that there is a stronger effect of Te migration from CdTe to CdS. We have also performed model calculations for changes of either CdS or CdTe layer thickness and also with Cd diffusion from CdTe to CdS, all these effects cannot account for the observed large changes in the angular dependence of Te FY.

For a quantitative comparison, the intensity of Te $K\alpha$ FY is divided by that of Cd $K\alpha$ and plotted as a function of the incidence angle in Fig. 3 for all the five samples. At high incidence angles (above 0.1°), where the x rays penetrate all the way through the sample, each of the ratio curves attains a more or less constant level, indicating an essentially constant concentration ratio of Te/Cd deep in the heterojunction. On the other hand, in the low-angle region (below 0.05°), where the x rays only penetrate to a shallow depth in the CdS layer, the Te/Cd FY ratio shows a strong dependence on the annealing temperature. Below 370 °C, the Te/Cd ratio in this low-angle region remains practically constant for a given annealing temperature except with some minor monotonic variations caused by the edge effect. Noticeably, for the samples annealed at 370 and 387 °C, the Te/Cd ratio at low angles jumps to higher values even above the high-angle level.

We propose a simple model to account for the changes in the Te $K\alpha$/Cd $K\alpha$ FY ratio from the low- to high-angle regions. Consider a glass/CdTe/CdS (''inverted'') bilayer system with a constant density of constituent atoms in each layer. Let $d_i$ and $\Phi_{A,i}$ be the layer thickness and constant density of element $A$ in the $i$th layer ($i = 1,2$ in the present case, referring to CdS and CdTe, respectively). We define the depth $z_0$ where the incident x ray has largely diminished such that the flux term $-dS_z(z)/dz$ becomes negligibly small when $z \geqslant z_0$. At low incident angles corresponding to $z_0 \leqslant d_1$, the Te $K\alpha$/Cd $K\alpha$ FY ratio is simply a constant:

TABLE I. Values of $R_1$, $R_2$, and $\Delta R/R_1$ for glass/200 Å–CdTe/200 Å–CdS inverted heterojunctions. $R_1$ is averaged over $\theta=0.02-0.05°$, and $R_2$ is averaged over $\theta=0.15-0.20°$.

| Annealing temperature (°C) | $R_1$ | $R_2$ | $\Delta R/R_1$ |
|---|---|---|---|
| No Annealing | $0.011\pm0.006$ | $0.592\pm0.008$ | $52.8\pm30.1$ |
| 340 | $0.073\pm0.008$ | $0.476\pm0.017$ | $5.52\pm0.95$ |
| 355 | $0.178\pm0.007$ | $0.448\pm0.003$ | $1.52\pm0.12$ |
| 360 | $0.344\pm0.021$ | $0.572\pm0.004$ | $0.663\pm0.11$ |
| 370 | $0.668\pm0.071$ | $0.484\pm0.001$ | $-0.275\pm0.14$ |
| 387 | $0.717\pm0.031$ | $0.515\pm0.003$ | $-0.282\pm0.059$ |

$$R_1=\frac{I_{\mathrm{Te}}}{I_{\mathrm{Cd}}}\propto\frac{\Phi_{\mathrm{Te},1}}{\Phi_{\mathrm{Cd},1}}. \tag{2}$$

For high incidence angles corresponding to $z_0\geqslant d_1+d_2$, this ratio now becomes

$$R_2=R_1\frac{C_1+C_2\Phi_{\mathrm{Te},2}/\Phi_{\mathrm{Te},1}}{C_1+C_2\Phi_{\mathrm{Cd},2}/\Phi_{\mathrm{Cd},1}}, \tag{3}$$

where

$$C_1=\int_0^{d_1}dz\left(-\frac{dS_z(z)}{dz}\right)\quad\text{and}\quad C_2=\int_{d_1}^{d_2}dz\left(-\frac{dS_z(z)}{dz}\right);$$

both remain constant for a given set of layer thickness and atomic density. The normalized difference of the ratios between low and high incidence angles can then be written as

$$\frac{\Delta R}{R_1}=\frac{R_2-R_1}{R_1}=\left(\frac{C_2}{C_1+C_2\Phi_{\mathrm{Cd},2}/\Phi_{\mathrm{Cd},1}}\right)\frac{\Phi_{\mathrm{Cd},2}}{\Phi_{\mathrm{Te},1}}\left(\frac{\Phi_{\mathrm{Te},2}}{\Phi_{\mathrm{Cd},2}}-\frac{\Phi_{\mathrm{Te},1}}{\Phi_{\mathrm{Cd},1}}\right). \tag{4}$$

From Eq. (2), the low-angle ratio $R_1$ is determined by the concentration ratio of Te/Cd in the first layer (CdS). And, from Eq. (4), the sign of the normalized ratio difference $(\Delta R/R_1)$ reflects the relative compositional change in each layer.

The ratios $R_1$, $R_2$, and $\Delta R/R_1$ are deduced from the FY data in Fig. 3 and listed in Table I. For simplicity, we have neglected any concentration gradient of Cd and Te in each layer, and assumed that the Te/Cd concentration ratio near the top surface of CdS can be approximated by a constant $R_1$, while that deep in the buried CdTe layer can be approximated by another constant $R_2$. Also, by neglecting the edge effect in each sample, the value of $R_1$ is obtained by averaging over $\theta=0.02-0.05°$. Likewise, $R_2$ is obtained by averaging over $\theta=0.15-0.20°$. From Table I we observe that: (a) The Te/Cd concentration ratio in the first (CdS) layer increases with annealing temperature for all the five samples, as shown by an increase of $R_1$ following Eq. (2). (b) According to Eq. (4), positive values of $\Delta R/R_1$ indicate that the Te/Cd concentration ratio in the second (CdTe) layer is higher than that in the first (CdS) layer for samples annealed at temperatures lower than 370 °C. (c) Negative values of $\Delta R/R_1$ suggest that the Te/Cd concentration ratio in the CdS layer has become larger than that in the CdTe layer in samples annealed at temperatures 370 °C and higher. Hence, migration of atoms in the inverted junctions (glass/CdTe/CdS) due to heating at 370 °C or higher temperatures could result in a strong intermixing of Te and Cd to the extent that the original window layer CdS can even behave somewhat like an absorber with a high Te/Cd ratio. Direct comparison with similar ADXRF spectra obtained with normal junctions (consisting of glass/CdS/CdTe) also confirms this conclusion.[8] We believe that although this analysis is based on an oversimplified model, the presence of a high Te/Cd ratio component in the CdS layer is clearly demonstrated in our experiment.

In conclusion, our ADXRF results show that a redistribution of both Cd and Te atoms has taken place in the inverted heterojunctions after thermal annealing. The heat treatment tends to reduce the original Te concentration contrast between CdS and CdTe layers and results in a blurred interface. When the annealing temperature exceeds a certain critical value such as 370 °C in our samples, an inverted junction can be transformed into a complicated admixture behaving like a normal junction near the CdS surface, as manifested by a Te/Cd concentration ratio higher than that in the CdTe layer. In a separate experiment we have found that the interfacial roughness at the CdS/CdTe interface also changes significantly with annealing temperature in these heterojunctions.[8] These results of *nondestructive* characterization of heterojunctions using ADXRF could, therefore, serve as useful tools for the control of atomic intermixing in the growth of thin-film photovoltaic materials.

The present research is supported by DOE and NREL. The authors are indebted to D. Grecu and X. Ma for assistance with the film deposition and to K. Makhratchev in the $CdCl_2$ anneals.

[1] C. Ferekides, J. Britt, Y. Ma, and L. Killian, *Proceedings of the 23th IEEE Photovoltaics Specialists Conference-1993* (IEEE, Piscataway, NJ, 1993), pp. 389–393.
[2] K. Zweibel, H. S. Ullal, and B. von Roedern, *Proceedings of the 25th IEEE Photovoltaics Specialists Conference-1996* (IEEE, Piscataway, NJ, 1996), pp. 745–750.
[3] P. V. Meyers, C. H. Liu, and T. J. Frey, U.S. Patent No. 4,710,589 (1987).
[4] A. Krol, C. Sher, and Y. H. Kao, Phys. Rev. B **38**, 8579 (1988).
[5] D. K. G. de Boer, Phys. Rev. B **44**, 498 (1991).
[6] M. Shao, A. Fischer, D. Grecu, U. Jayamaha, E. Bykov, G. Contreras-Puente, R. G. Bohn, and A. D. Compaan, Appl. Phys. Lett. **69**, 3045 (1996).
[7] Y. L. Soo, S. Huang, Y. H. Kao, and A. D. Compaan, J. Appl. Phys. **83**, 4173 (1998).
[8] S. Huang, Y. L. Soo, Y. H. Kao, and A. D. Compaan (unpublished).